Bioorganic & Medicinal Chemistry 18 (2010) 567–572

Contents lists available at ScienceDirect

Bioorganic & Medicinal Chemistry

journal homepage: www.elsevier.com/locate/bmc

Synthesis of 6-*N*-(benzothiazol-2-yl)deoxyadenosine and its exciton-coupled circular dichroism

Yoshiaki Masaki, Akihiro Ohkubo, Kohji Seio, Mitsuo Sekine *

Department of Life Science, Tokyo Institute of Technology, 4259 Nagatsuta, Midori-ku, Yokohama 226-8501, Japan

ARTICLE INFO

Article history:
Received 19 October 2009
Revised 2 December 2009
Accepted 3 December 2009
Available online 11 December 2009

Keywords:
Exciton coupling
Circular dichroism
Modified nucleic acid
Benzothiazole

ABSTRACT

6-*N*-(Benzothiazol-2-yl)deoxyadenosine (A^{BT}) was synthesized and incorporated into DNAs. Although, the multipoint benzothiazole (BT) modification of oligodeoxynucleotides reduced the stability of duplexes with their complementary strands, it induced the strong exciton coupling between BT moieties. The circular dichroism (CD) spectra of this exciton coupling interaction were observed at wavelengths above 300 nm and overlapping with the UV absorption bands of nucleotides could be avoided. The shapes of the CD spectra due to this interaction were strongly influenced by the helicity of two BT groups.

1. Introduction

Circular dichroism (CD) spectra are widely used to study conformation of DNAs and their changes.[1–3] The conformational change of DNAs was observed below 300 nm in their CD spectra. However, the presence of other forms of DNAs or the binding with other UV-active biomolecules makes it difficult to detect the change of local conformation.[4–6] To overcome this problem, the chiroptical probes that absorb above 300 nm were desired. The porphyrins[4–6] and stilbene[7–9] were well known as the exciton-coupled CD (ECCD) probes that absorb above 300 nm, and the porhyrins were used as probes for the B–Z transition of DNAs.[6] These chromophores were attached to the terminal position of DNA strands. However, there is no paper to incorporate such chromophores into the intra-strand position to investigate the local conformation change of long DNA by ECCD. In this case, the chromophore should not cause to distort the duplex and should have an exciton coupling property at wavelengths above 300 nm to avoid the effect of the UV absorbance bands of the nucleobases.

The benzothiazole moiety usually gives UV absorption bands above 300 nm and has been used to attach optical properties to biomolecules.[10–12] Because benzothiazole derivatives were often used as the intercalators, it was expected that a benzothiazole (BT)-modified adenine base could be used like a universal base with the minimum distortion on DNA duplex structures. In addition, 6-*N*-modification of the adenine moiety could be attained using the Buchwald–Hartwig reaction. Herein, we report the convenient synthesis of 6-*N*-(benzothiazol-2-yl)deoxyadenosine (A^{BT}) and unique properties of its exciton-coupled circular dichroism upon incorporation into DNA oligomers.

2. Results and discussion

2.1. Synthesis of 6-*N*-(benzothiazol-2-yl)deoxyadenosine and its derivatives

The synthesis of 6-*N*-(benzothiazol-2-yl)deoxyadenosine (**3**) is shown in Scheme 1. The reaction of compound **1**[13] with 2-aminobenzothiazole in the presence of $Pd(dba)_2$, Xantphos, and Cs_2CO_3 at 80 °C produced the N-arylated product **2** in 93% yield. Treatment of compound **2** with 3HF·TEA produced the deprotected product **3** in 89% yield. Compound **3** was converted to the phosphoramidite derivatives **4** in 72% yield (two steps) by the successive 5′-*O*-dimethoxytritylation and 3′-phosphytilation. The synthesis of oligonucleotides was performed according to the phosphoramidite approach using an ABI 392 DNA/RNA automated synthesizer. The base sequences of the synthesized oligodeoxynucleotides are summarized in Figure 1.

2.2. Properties of modified oligonucleotides (ODN1, ODN21, ODN22, and ODN3)

2.2.1. UV spectra of single stranded oligodeoxynucleotides modified with A^{BT}

The normalized UV spectra of the modified oligodeoxynucleotides (ODNs) are shown in Figure 2. To compare the unmodified

* Corresponding author. Tel.: +81 45 924 5706; fax: +81 45 924 5772.
E-mail address: msekine@bio.titech.ac.jp (M. Sekine).

0968-0896/$ - see front matter © 2009 Elsevier Ltd. All rights reserved.
doi:10.1016/j.bmc.2009.12.009

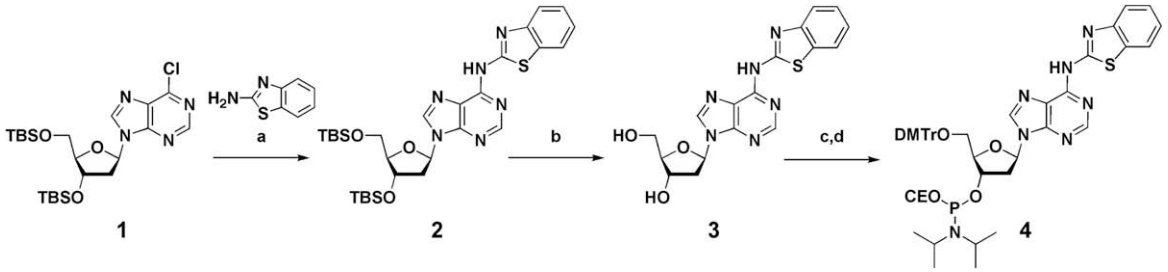

Scheme 1. Reagents and conditions: (a) 2-aminobenzothiazole, 5 mol % $Pd(dba)_2$, 10 mol % Xantphos, Cs_2CO_3, 1,4-dioxane, 80 °C, 3 h, 93%; (b) 3HF·TEA, TEA, THF, rt, 16 h, 89%; (c) DMTrCl, pyridine, rt, 12 h, 89%; (d) (CEO)P($NiPr_2$)$_2$, 1*H*-tetrazole, *i*Pr_2NH, CH_2Cl_2, rt, 2.5 h, 80%.

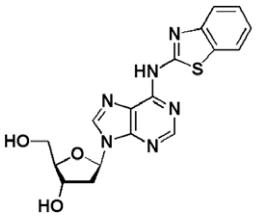

A^{BT}: 6-*N*-(benzothiazol-2-yl)deoxyadenosine

synthesized sequence

ODN1	5′-dTA CCTA A^{BT}A TCCAT-3′
ODN21	5′-dTA CCT $A^{BT}A^{BT}$A TCCAT-3′
ODN22	5′-dTA^{BT}CCTA A^{BT}A TCCAT-3′
ODN3	5′-dTA CCT $A^{BT}A^{BT}A^{BT}$TCCAT-3′
A1	5′-dGGC $A^{BT}A^{BT}$A A A A CGG-3′
A2	5′-dGGC A^{BT}A A^{BT}A A A CGG-3′
A3	5′-dGGC A^{BT}A A A^{BT}A A CGG-3′
A4	5′-dGGC A^{BT}A A A A^{BT}A CGG-3′
A5	5′-dGGC A^{BT}A A A A A^{BT}CGG-3′
A6	5′-dA^{BT}GGCA A A A A A CGG A^{BT}-3′

Figure 1. 6-*N*-(Benzothiazol-2-yl)deoxyadenosine and base sequences of oligodeoxynucleotides incorporating this modified nucleoside.

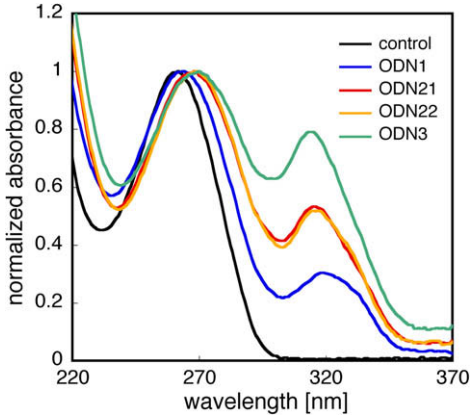

Figure 2. Normalized UV spectra of modified oligodeoxynucleotides containing A^{BT}. The sequence of **ODN1**: 5′-d(TACCTAA^{BT}ATCCAT), **ODN21**: 5′-d(TACCTA$^{BT}A^{BT}$ATCCAT), **ODN22**: 5′-d(TA^{BT}CCTAA^{BT}ATCCAT), ODN3: 5′-d(TACCTA$^{BT}A^{BT}A^{BT}$TCCAT). The control means unmodified oligodeoxynucleotide: 5′-d(TACCTAAATCCAT).

ODN (**control**) with a one-point BT modified ODN (**ODN1**), the additional absorption of the BT moiety was observed at a 300–350 nm region. The UV intensities of two-point BT modified ODNs (**ODN21** and **ODN22**) and a three-point BT modified ODN (**ODN3**) in 300–350 nm region were increased proportionally with an increase in the number of BT moieties.

2.2.2. Hybridization properties of multi-modified DNAs

The hybridization properties of BT modified oligodeoxynucleotides toward the target DNA were determined by measuring the melting temperature (T_m) values from the temperature-dependent UV profiles of the duplexes with their complementary oligodeoxynucleotides. The T_m value of **ODN1** with a target strand (Y = T) was 39.3 °C and that of the control duplex was 43.6 °C (Table 1). This means that incorporation of the A^{BT} moiety into DNA destabilized the thermal stability of the resulting duplex. On the other hand, the T_m values of three mismatch strands with **ODN1** were 37.2 °C for A^{BT}:G (29.9 °C for A:G), 36.5 °C for A^{BT}:A (26.5 °C for A:A), and 41.7 °C for A^{BT}:C (27.3 °C for A:C). The base-recognition ability was determined by the difference in T_m value between the match and mismatch duplexes. The base-recognition ability of **ODN1** strand was only +2.4 to −2.8 °C and control strand was −13.7 to −17.1 °C. It seems that the A^{BT} was not paired with the counterpart base.

2.2.3. CD spectra of duplexes with A^{BT}

To clarify the influence of the BT moiety on the duplex structure, the CD spectra of the modified and unmodified duplexes were measured (Fig. 3). Their spectra were almost similar in the region of 220–300 nm without relatively stronger positive cotton effects in 260–300 nm. It should be noted that there were almost no signals at 300–350 nm where the UV absorption bands arising from the BT moiety were observed.

Next, we measured the CD spectra of the multi-modified duplexes of **ODN21**, **ODN22**, and **ODN3** with their complementary strands. These results are summarized in Figure 4. Interestingly, the multi-modification of the BT moiety induced new circular dichroism signals in the 300–350 nm region, which was not observed in the duplex containing **ODN1**. In addition, although there

Table 1
The base-recognition ability of A^{BT}

Entry	X[a]	Y[b]	T_m[c] (°C)	ΔT_m[d] (°C)
1	A^{BT}	T	39.3	—
2		G	37.2	−2.1
3		A	36.5	−2.8
4		C	41.7	+2.4
5	A	T	43.6	—
6		G	29.9	−13.7
7		A	26.5	−17.1
8		C	27.3	−16.3

[a] 5′-d(TACCTAXATCCAT)3′, **ODN1** (X = A^{BT}), Control (X = A).
[b] 5′-d(ATGGATYTAGGTA)-3′.
[c] T_m values were measured in 10 mM sodium phosphate buffer (pH 7.0), containing 0.1 M NaCl, 0.1 mM EDTA, 2.0 μM of each oligomer.
[d] $\Delta T_m = T_m - T_m^{Y=T}$.

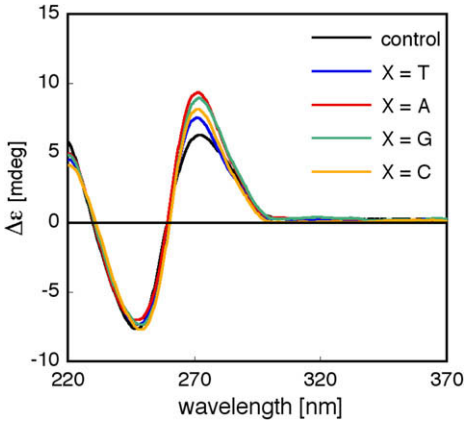

Figure 3. Circular dichroism spectra of 5′-d(TACCTAA^{BT}ATCCAT)/5′-d(ATGGATX TAGGTA) duplexes (X = T, G, A, or C) at 10 °C in 10 mM sodium phosphate buffer (pH 7.0), containing 0.1 M NaCl, 0.1 mM EDTA, 5.0 μM of each oligomer. The control means unmodified duplex.

are the only two or three BT moieties in the 13 mer duplex (total 26 nucleobases), the intensities of CD spectra in the 300–350 nm region were comparable with those in the region of 220–300 nm, which was originated from the nucleobases. These results indicated that the exciton coupling existed between the BT moieties.

The duplex of **ODN21** with the complementary oligomer showed a positive Cotton effect at 320–350 nm and a negative Cotton effect at 300–320 nm. The modification did not affect the CD signal in the nucleobase region (220–300 nm). The shape of the CD spectrum at 300–350 nm was quite similar to that observed in the nucleobase region. This suggested that the BT moieties were aligned along the helical geometry. Interestingly, the duplex containing **ODN22** showed a negative Cotton effect at 320–340 nm and a positive Cotton effect at 300–320 nm, which is opposite to the spectrum of the **ODN21**-containing duplex. This phenomenon was agreed with the previous studies.[7–9] An important factor of the intensity of the Cotton effect is the angle (θ) between the electronic transition dipole moments of two chromophores. The effect of the angle was expressed by the following formula:[8]

$$\Delta\varepsilon \approx \pm\frac{\pi}{4\lambda}\mu_i^2\mu_j^2 R_{ij}^{-2}\sin(2\theta),$$

where μ_i and μ_j are the transition dipole moments of the two chromophores and R_{ij} is the distance between them. The angle (θ) of **ODN21** was expected to be near the twist value (36°) of the standard B-form base-pair step and that of **ODN22** was expected to be near 180°, that is, fivefold wider than the twist of the base-pair step. The mirror image CD shape suggested that the angle (θ) between the chromophores was below 180°.

The **ODN3** duplex also showed a significant positive Cotton effect at 317–350 nm, a negative Cotton effect at 300–317 nm, and the same shape as that of the nucleobase region. The intensity of the BT region (300–350 nm) was increased, but that of the nucleobase region (220–300 nm) was decreased. This result suggests that the consecutive three-point BT modification would destabilize the whole duplex structure and the Cotton effect due to the right-handed helical structure of three benzothiazoles was markedly observed. Thus, the two-point BT modification is more suitable for the detection of local conformation change.

2.3. Properties of modified oligonucleotides (A1–A6)

2.3.1. Hybridization properties of two-point modified DNAs

Next, we studied the dependency of the distance and helicity between BT moieties. The base sequences and T_m values of the modified oligonucleotides synthesized in this study are summarized in Table 2. Consequently, the DNA oligomer (**A1**) with a consecutively arranged $A^{BT}A^{BT}$ sequence showed the T_m value of 42.0 °C that was lower by 8.2 °C than the unmodified oligomer, when hybridized with the complementary DNA oligomer. The duplexes involving dispersedly modified oligomers (**A2–A5**) showed the T_m values of 45.6, 46.6, 44.4, and 40.2 °C, respectively. The duplex of the dangling-end modified oligomer (**A6**) with the same complementary DNA oligomer showed the T_m value of 59.5 °C. The additional stabilizing effect (+9.3 °C) of this duplex could be explained by the stacking effect of the dangling-end modified nucleobase.[14]

Table 2
The melting temperature of two-point A^{BT} modified ODNs

Entry		Sequence	T_m[a] (°C)	ΔT_m[b] (°C)
1	A1	5′-d(GGCA^{BT}A^{BT}AAAACGG)	42.0	−8.2
2	A2	5′-d(GGCA^{BT}AA^{BT}AAACGG)	45.6	−4.6
3	A3	5′-d(GGCA^{BT}AAA^{BT}AACGG)	46.6	−3.6
4	A4	5′-d(GGCA^{BT}AAAA^{BT}ACGG)	44.4	−5.8
5	A5	5′-d(GGCA^{BT}AAAAA^{BT}CGG)	40.2	−10.0
6	A6	5′-d(A^{BT}GGCAAAAAAACGGA^{BT})	59.5	+9.3
7	Control	5′-d(GGCAAAAAACGG)	50.2	—

[a] T_m values were measured in 10 mM sodium phosphate buffer (pH 7.0), containing 0.1 M NaCl, and 0.1 mM EDTA, 2.0 μM of each oligomer.
[b] $\Delta T_m = T_m - T_m^{control}$.

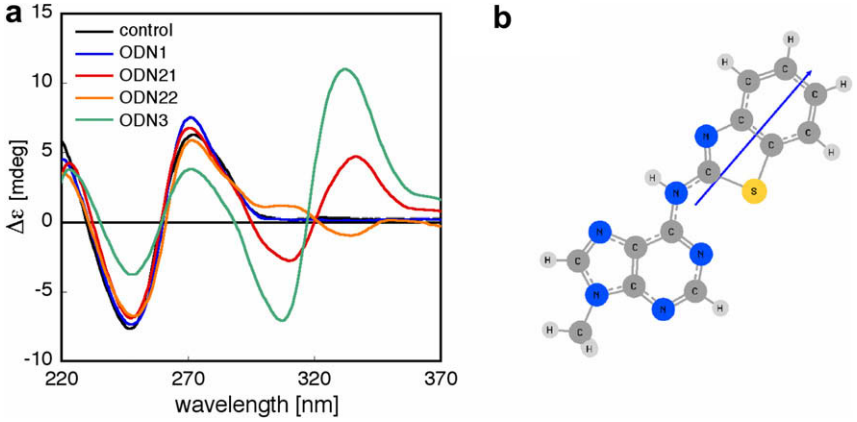

Figure 4. (a) Circular dichroism spectra of the duplexes containing **ODN1**, ODN2, and ODN3 strands at 10 °C in 10 mM sodium phosphate buffer (pH 7.0), containing 0.1 M NaCl, and 0.1 mM EDTA, 5.0 μM of each oligomer. The control means unmodified duplex. (b) The direction of transition dipole moment of the A^{BT} analogue was calculated at the TDDFT/B3LYP/6-31+G(d,p) level by using GAUSSIAN03.[15]

2.3.2. Dependency of the helicity between BT moieties

Figure 5 shows the CD spectra of the duplexes of **A1**–**A6** with the complementary DNA 12 mer. The **A1** duplex with consecutively two-point modified bases showed a strong Cotton effect at 320–350 nm and a relatively weak negative Cotton effect at 300–320 nm. The CD intensity at 300–350 nm was comparable with that of the nucleobase region. The CD spectrum of the **A2** duplex having an $A^{BT}AA^{BT}$ sequence was similar to that of the **A1** duplex except for the blue shift of the maximum of the positive Cotton effect at 320–350 nm (from 337 nm (**A1**) to 333 nm (**A2**)).

Surprisingly, the shapes of the CD spectra of the **A3** and **A4** duplexes with two and three deoxyadenosines (As) between two A^{BT} deoxynucleosides were changed. The **A3** and **A4** duplexes showed only the positive Cotton effect at 300–350 nm region and the negative Cotton effect disappeared. The maxima of the positive Cotton effect were blue shifted (326 nm for **A3** and 321 nm for **A4** duplex). In addition, the shapes of the CD spectra of the **A3** and **A4** duplexes also changed in the nucleobase region (220–300 nm), especially at 260–280 nm. The NMR study of this sequence showed that the middle part of this sequence forms the A-tract structure.[16] This change of the nucleobase region suggests that the BT moieties incorporated in the mid-part of the A-tract sequence interfered with the formation of the A-tract structure, possibly causing the change in the orientation of the BT moieties. These factors might cause the unusual behavior of CD spectra.

Interestingly, the **A5** duplex with four deoxyadenosines inserted between two A^{BT} nucleosides showed almost no Cotton effect at 300–350 nm. The angle (θ) between the BT moieties in **A5** duplex is expected to be approximately 182°, which was the sum of the twist angles of base-pair step parameters of the NMR structure (PDB: 1FZX).[16] As discussed above (Section 2.2.3), the intensity of the CD spectrum is proportional to $\sin(2\theta)$. Thus, the **A5** duplex would have almost no signal of the Cotton effect.

The **A6** duplex still showed the Cotton effect. A negative Cotton effect was observed at 300–350 nm (negative absorption minimum at 327 nm). The BT moiety could show the ECCD spectra even when separated by 12 base pairs. It is said that the intensity of interaction between chromophores decreases sharply with an increase in the distance. For example, the intensity of fluorescence resonance energy transfer (FRET) and photo-induced electron transfer (PET) decreased with an increase in distance R ($1/R$,[6] and exp ($1/R$), respectively).[7,17,18] Our results indicate that the ECCD spectra were also a powerful tool to observe the long-distance interaction.

3. Conclusions

We synthesized the 6-*N*-(benzothiazol-2-yl)deoxyadenosine (A^{BT}) and clarified its property of exciton-coupled circular dichroism (ECCD). Although the benzothiazole (BT) moiety destabilizes the thermal stability of duplexes, the CD spectra indicated that the BT moiety does not markedly distort the duplex structure. In addition, multipoint BT modifications induced strong ECCD at the 300–350 nm region, which was not overlapped with the absorption region of nucleotidic UV bands. The shapes of CD spectra were strongly influenced by the helicity of benzothiazole chromophores.

4. Experimental procedures

4.1. General remarks

The dry solvents were purchased and stored over molecular sieves 4A. ^{1}H, ^{13}C, and ^{31}P NMR spectra were obtained at 500, 126, and 203 MHz, respectively. The chemical shifts were measured from $CDCl_3$ (7.26 ppm), DMSO-d_6 (2.50 ppm) for ^{1}H NMR, $CDCl_3$ (77.0 ppm), DMSO-d_6 (39.5 ppm) for ^{13}C NMR and 85% phosphoric acid (0.0 ppm) for ^{31}P NMR. UV spectra were recorded with a U-2810 spectrometer. Column chromatography was performed with silica gel C-200 (purchased from Wako Co. Ltd). High performance liquid chromatography (HPLC) was performed using the following systems: Reversed exchange HPLC was done on a Waters Alliance system with a Waters 3D UV detector and a Waters XTerra MS C18 column (4.6 × 150 mm); a linear gradient (0–30%) of solvent I (0.1 M ammonium acetate buffer (pH 7.0)) in solvent II (CH_3CN) was used at 50 °C at a flow rate of 1.0 mL/min for 30 min; anion-exchange HPLC was done on a Shimadzu LC-10 AD VP with a Shimadzu 3D UV detector and a Gen-Pak FAX column (Waters, 4.6 × 100 mm); a linear gradient (10–67%) of solvent III (1 M NaCl in 25 mM phosphate buffer (pH 6.0)) in solvent IV (25 mM phosphate buffer (pH 6.0)) was used at 50 °C at a flow rate of 1.0 mL/min for 40 min. ESI mass was performed using Mariner™ (PerSeptive Biosystems Inc.). MALDI-TOF mass was performed using a Bruker Daltonics (Matrix: 3-hydoroxypicolinic acid (100 mg/mL) in H_2O-diammoniumhydrogen citrate (100 mg/mL) in H_2O (10 : 1, v/v)).

4.2. Synthesis of phosphoramidite unit

4.2.1. 3′,5′-Di-*tert*-butyldimehylsilyl-6-*N*-(benzothiazoyl-2-yl)-deoxyadenosine 2

$Pd(dba)_2$ (57.8 mg, 0.1 mmol) and Xantphos (116 mg, 0.2 mmol) were dissolved in dry 1,4-dioxane (20 mL). The mixture was stirred at room temperature for 30 min. To the solution were added Cs_2CO_3 (982 mg, 3.01 mmol), 2-aminobenzothiazole (603 mg, 4.02 mmol), and compound **1** (1.00 g, 2.01 mmol) in dry 1,4-dioxane (20 mL). After being stirred at 80 °C for 3 h, the mixture was filtered using Celite. The solvent was evaporated in vacuo and the residue was chromatographed on a silica gel column with $CHCl_3$–MeOH (99:1,

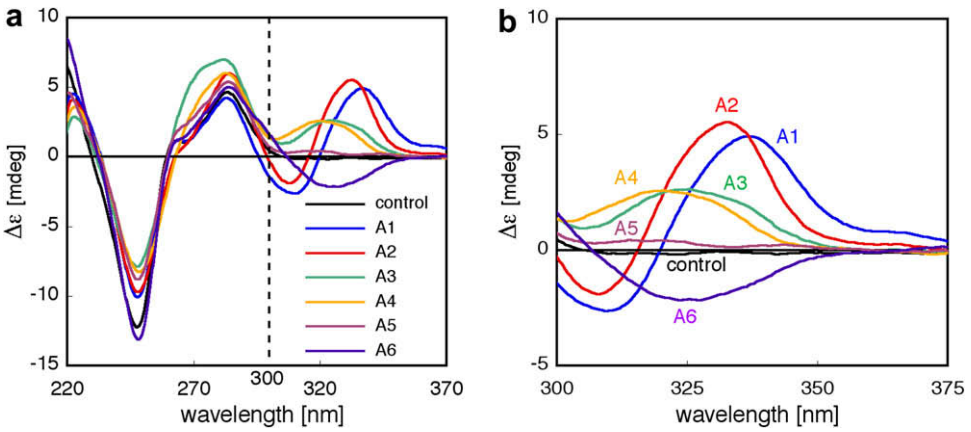

Figure 5. Circular dichroism spectra at 10 °C in 10 mM sodium phosphate buffer (pH 7.0), containing 0.1 M NaCl, and 0.1 mM EDTA, 5.0 μM of each oligomer.

v/v) to give compound **2** as pale yellow oil (1.11 g, 93%): ^{1}H NMR ($CDCl_3$, 500 MHz): δ 8.72 (1H, s), 8.38 (1H, s), 7.83 (1H, d, J = 7.5), 7.80 (1H, d, J = 7.5), 7.43 (1H, t, J = 7.5), 7.29 (1H, t, J = 7.5), 6.52 (1H, t, J = 6.0), 4.65–4.62 (1H, m), 4.04 (1H, d, J = 3.5), 3.88 (1H, dd, J = 3.5, 11.0), 3.78 (1H, dd, J = 3.0, 11.0), 2.68 (1H, dt, J = 6.0,12.5), 2.49 (1H, ddd, J = 3.5, 6.0, 12.5) 0.92 (9H, s), 0.91 (9H, s), 0.11 (6H, s), 0.08 (6H, s); ^{13}C NMR ($CDCl_3$, 126 MHz): δ 158.3, 151.5, 150.2, 149.0, 148.6, 141.7, 133.2, 125.9, 123.2, 121.0, 120.8, 120.6, 88.1, 84.7, 72.0, 62.8, 41.1, 25.8, 25.7, 18.3, 18.0, −4.7, −4.8, −5.5, −5.6; MS (ESI) calcd for $C_{29}H_{44}N_6O_3SSi_2$ $[M+H]^+$ 613.2807, found 613.2837.

4.2.2. 6-*N*-(Benzothiazoyl-2-yl)deoxyadenosine 3

Compound **2** (1.11 g, 1.81 mmol) was dissolved in dry THF (20 mL). To the solution were added $Et_3N{\cdot}3HF$ (0.59 mL, 3.62 mmol) and triethylamine (0.51 mL, 3.62 mmol). After being stirred at room temperature for 16 h, the reaction mixture was filtered. The residue was dissolved in pyridine and precipitated by $CHCl_3$ to give compound **3** as a pale yellow solid (0.618 g, 89%): ^{1}H NMR (DMSO, 500 MHz): δ 12.45 (1H, br s), 8.67 (1H, s), 8.65 (1H, s), 7.95 (1H, d, J = 7.5), 7.68 (1H, d, J = 7.5), 7.41 (1H, t, J = 7.5), 7.26 (1H, t, J = 7.5), 6.46 (1H, t, J = 6.5), 5.36 (1H, br s), 5.05 (1H, br s), 4.44 (1H, br s), 3.90 (br s, 1H), 3.65–3.62 (1H, m), 3.55–3.52 (1H, m), 2.77 (1H, dt, J = 6.5, 13.0), 2.37–2.32 (1H, m); ^{13}C NMR (DMSO, 126 MHz): δ 150.7, 150.3, 142.0, 126.1, 122.9, 121.4, 88.0, 83.8, 70.7, 61.6; MS (ESI) calcd for $C_{17}H_{16}N_6O_3S$ $[M+H]^+$ 385.1077, found 385.1091.

4.2.3. 5′-*O*-(4,4′-Dimethoxytrityl)-6-*N*-(benzothiazoyl-2-yl)deoxyadenosine 3a

Compound **3** (0.716 g, 1.86 mmol) was co-evaporated three times with dry pyridine and finally dissolved in dry pyridine (20 mL). To the solution was added 4,4′-dimethoxytrityl chloride (0.757 g, 2.24 mmol). After being stirred at room temperature for 12 h, the mixture was quenched by adding methanol and evaporated in vacuo. The residue was dissolved with $CHCl_3$. The solution was washed with water. The organic layer was concentrated in vacuo. The residue was chromatographed on a column of silica gel with $CHCl_3$–MeOH (95:5, v/v) containing 0.5% pyridine to give compound **3a** as white foam (1.144 g, 89%): ^{1}H NMR ($CDCl_3$, 500 MHz): δ 11.2 (1H, br s), 8.66 (1H, s), 8.55 (1H, s), 7.84 (1H, d, J = 8.0), 7.74 (1H, d, J = 8.0), 7.10–7.40 (11H, m), 6.69–6.76 (4H, m), 6.57 (1H, t, J = 6.0), 4.78 (1H, d, J = 3.5), 4.26–4.32 (1H, m), 3.70 (6H, s), 3.44–3.51 (1H, m), 3.38–3.44 (1H, m), 2.96 (1H, dt, J = 6.5, 13.0), 2.64–2.72 (1H, m); ^{13}C NMR ($CDCl_3$, 126 MHz): δ 158.5, 158.4, 151.3, 150.1, 148.8, 148.6, 144.4, 141.9, 135.6, 135.5, 133.0, 129.9, 129.9, 128.0, 127.7, 126.8, 125.9, 123.1, 120.9, 120.7, 120.5, 113.0, 86.5, 86.1, 84.6, 72.3, 63.6, 55.1, 39.9; MS (ESI) calcd for $C_{38}H_{35}N_6O_5S$ $[M+H]^+$ 687.2384, found 687.2347.

4.2.4. 3′-*O*-[(*N*,*N*-Diisopropylamino)-2-cyanoethoxyphosphinyl]-5′-*O*-(4,4′-dimethoxytrityl)-6-*N*-(benzothiazoyl-2-yl)deoxyadenosine 4

Compound **3a** (671 mg, 0.98 mmol) was dissolved in dry CH_2Cl_2 (10 mL). To the solution were added diisopropylamine (82.4 μL, 0.58 mmol) and bis-(*N*,*N*-diisopropylamino)(2-cyanoethoxy)phosphine (324 μL) in dry CH_2Cl_2 (10 mL). After being stirred at room temperature for 2.5 h, the mixture was washed with saturated $NaHCO_3$ solution. The organic layer was evaporated in vacuo. The residue was chromatographed on a column of silica gel with $CHCl_3$–MeOH (97:3, v/v) containing 0.5% pyridine to give compound **4** as white foam (692 mg, 80%): ^{1}H NMR ($CDCl_3$, 500 MHz): δ 8.67 (1H, s), 8.54–8.64 (1H, m), 7.85 (1H, d, J = 7.0), 7.75 (1H, d, J = 7.5), 7.30–7.40 (11H, m), 6.69–6.81 (4H, m), 6.48–6.56 (1H, br s), 4.78–4.8 (1H, m), 4.32–4.42 (1H, m), 3.50–3.92 (10H, m), 3.34–3.48 (2H, m), 2.98–3.09 (1H, m), 2.58–2.82 (2H, m), 2.44–2.53 (1H, m), 1.13–1.38 (12H, m); ^{13}C NMR ($CDCl_3$, 126 MHz): δ 158.4, 151.3, 150.2, 148.9, 148.7, 144.5, 142.2, 142.1, 135.6, 133.1, 130.0, 129.9, 128.1, 128.0, 127.7, 126.8, 125.9, 123.1, 120.9, 120.5, 117.5, 117.4, 113.0, 86.3, 86.0, 85.8, 85.8, 84.9, 74.2, 74.0, 73.5, 73.3, 63.5, 63.3, 58.4, 58.2, 58.1, 55.1, 45.3, 45.2, 44.4, 44.4, 43.3, 43.2, 39.1, 24.6, 24.5, 24.5, 24.4, 23.6, 22.9, 22.8, 22.6, 20.3, 20.3, 20.2, 20.1, 20.0, 19.9; ^{31}P NMR ($CDCl_3$) δ 149.4, 149.3; MS (ESI) calcd for $C_{47}H_{52}N_8O_6PS$ $[M+H]^+$ 887.3463, found 887.3445.

4.3. Synthesis of oligonucleotides

The synthesis of ODNs was performed in an ABI 392 DNA synthesizer by the standard 1.0-μmol-scale phosphoramidite approach, which consists of detritylation, coupling, capping, and iodine oxidation steps. The universal supports III (Glen Research Inc.) was used for the synthesis of the **A6** sequence. Then, the synthesized oligomers were released from the resin by treatment with a solution of 28% aq NH_3 solution at room temperature for 4 h. The polymer supports were removed by filtration and washed with 0.1 M ammonium acetate buffer (1 mL × 3). The filtrates were purified by anion-exchange HPLC to give ODNs.

Oligonucleotide: **ODN1**: MALDI-TOF Mass (M+H) calcd for $C_{133}H_{165}N_{46}O_{75}P_{12}S^+$: 4009.2; found: 4006.0.

Oligonucleotide: **ODN21**: MALDI-TOF Mass (M+H) calcd for $C_{140}H_{168}N_{47}O_{75}P_{12}S_2^+$: 4142.7; found: 4139.6.

Oligonucleotide: **ODN22**: MALDI-TOF Mass (M+H) calcd for $C_{140}H_{168}N_{47}O_{75}P_{12}S_2^+$: 4142.7; found: 4137.0.

Oligonucleotide: **ODN3**: MALDI-TOF Mass (M+H) calcd for $C_{147}H_{171}N_{48}O_{75}P_{12}S_3^+$: 4275.7; found: 4273.4.

Oligonucleotide: **A1**: MALDI-TOF Mass (M+H) calcd for $C_{132}H_{152}N_{58}O_{64}P_{11}S_2^+$: 3977.7; found: 3972.9.

Oligonucleotide: **A2**: MALDI-TOF Mass (M+H) calcd for $C_{132}H_{152}N_{58}O_{64}P_{11}S_2^+$: 3977.7; found: 3978.0.

Oligonucleotide: **A3**: MALDI-TOF Mass (M+H) calcd for $C_{132}H_{152}N_{58}O_{64}P_{11}S_2^+$: 3977.7; found: 3974.5.

Oligonucleotide: **A4**: MALDI-TOF Mass (M+H) calcd for $C_{132}H_{152}N_{58}O_{64}P_{11}S_2^+$: 3977.7; found: 3972.7.

Oligonucleotide: **A5**: MALDI-TOF Mass (M+H) calcd for $C_{132}H_{152}N_{58}O_{64}P_{11}S_2^+$: 3977.7; found: 3976.0.

Oligonucleotide: **A6**: MALDI-TOF Mass (M+H) calcd for $C_{152}H_{176}N_{68}O_{74}P_{13}S_2^+$: 4603.8; found: 4599.7.

4.4. T_m measurement

The unmodified oligodeoxynucleotides were purchased from SIGMA GENOSYS. An appropriate ODN (2 μM) and its complementary ssDNA (2 μM) were dissolved in a buffer consisting of 100 mM NaCl, 10 mM sodium phosphate, and 0.1 mM EDTA adjusted to pH 7.0. The solution was kept at 85 °C for 10 min for complete dissociation of the duplex to single strands, cooled at the rate of −1.0 °C/min, and kept 10 °C for 10 min. Then, the melting temperatures (T_m) were determined at 260 nm using a UV spectrometer (Pharma Spec UV-1700™, Shimadzu) by increasing the temperature at the rate of 1.0 °C/min.

4.5. CD spectra

CD spectra were measured on J-725 Spectroplarimeter, JASCO. Each oligodeoxynucleotide solutions (5 μM)) were prepared in 10 mM sodium phosphate buffer pH 7.0, 0.1 mM EDTA, and 100 mM NaCl. The solutions were heated to 85 °C and annealed by slowly cooling to room temperature over a period of 12 h. Spectra were recorded between 220 and 370 nm. Spectra were averaged over 8 scans, which were recorded at 100 nm min^{-1} with a response time of 4 s and a bandwidth of 1.0 nm.

4.6. Computational method

The structure of the 6-*N*-benzothiazolyl adenine analogue was optimized at the B3LYP/6-31+G(d,p) level by using the GAUSSIAN03 software.[15] The vibrational frequency was calculated to confirm the equilibrium geometries that correspond to energy the minimum. After that, the excited state calculation was performed on the optimized structure at the TDDFT/B3LYP/6-31+G(d,p) level. The direction of the transition dipole moment was depicted by using the GaussView.

Acknowledgments

This work was supported by a grant from Grant-in-Aid for Scientific Research from the Ministry of Education, Culture, Sports, Science and Technology, Japan and in part by Health Sciences Research Grants for Research on Psychiatric and Neurological Diseases and Mental Health from the Ministry of Health, Labor and Welfare of Japan, and by the global COE project.

References and notes

1. Muhuri, S.; Mimura, K.; Miyoshi, D.; Sugimoto, N. *J. Am. Chem. Soc.* **2009**, *131*, 9268.
2. Schonhoft, J. D.; Bajracharya, R.; Dhakal, S.; Yu, Z.; Mao, H.; Basu, S. *Nucleic Acids Res.* **2009**, *37*, 3310.
3. Westrate, L.; Mackay, H.; Brown, T.; Nguyen, B.; Kluza, J.; David Wilson, W. D.; Lee, M.; Hartley, J. A. *Biochemistry* **2009**, *48*, 5679.
4. Balaz, M.; Holmes, A. E.; Benedetti, M.; Rodriguez, P. C.; Berova, N.; Nakanishi, K.; Proni, G. *J. Am. Chem. Soc.* **2005**, *127*, 4172.
5. Balaz, M.; Bitsch-Jensen, K.; Mammana, A.; Ellestad, G. A.; Nakanishi, K.; Berova, N. *Pure Appl. Chem.* **2007**, *79*, 801.
6. Balaz, M.; Li, B. C.; Steinkruger, J. D.; Ellestad, G. A.; Nakanishi, K.; Berova, N. *Org. Biomol. Chem.* **2006**, *4*, 1865.
7. Lewis, F. D.; Liu, X.; Wu, Y.; Zuo, X. *J. Am. Chem. Soc.* **2003**, *125*, 12729.
8. Lewis, F. D.; Zhang, L.; Liu, X.; Zuo, X.; Tiede, D. M.; Long, H.; Schatz, G. C. *J. Am. Chem. Soc.* **2005**, *127*, 14445.
9. Burin, A. L.; Armbruster, M. E.; Hariharan, M.; Lewis, F. D. *Proc. Natl. Acad. Sci. U.S.A.* **2009**, *106*, 989.
10. Ono, M.; Hayashi, S.; Kimura, H.; Kawashima, H.; Nakayama, M.; Saji, H. *Bioorg. Med. Chem.* **2009**, *17*, 7002.
11. Abbotto, A.; Beverina, L.; Bozio, R.; Facchetti, A.; Ferrante, C.; Pagani, G. A.; Pedron, D.; Signorini, R. *Org. Lett.* **2002**, *4*, 1495.
12. Mashraqui, S. H.; Kumar, S.; Vashi, D. *J. Inclusion Phenom. Macrocycl. Chem.* **2004**, *48*, 125.
13. Dai, Q.; Ran, C.; Harvey, R. G. *Org. Lett.* **2005**, *7*, 999.
14. Isaksson, J.; Chattopadhyaya, J. *Biochemistry* **2005**, *44*, 5390.
15. Frisch, M. J.; Trucks, G. W.; Schlegel, H. B.; Scuseria, G. E.; Robb, M. A.; Cheeseman, J. R.; Zakrzewski, V. G.; Montgomery, J. A.; Stratmann, R. E.; Burant, J. C.; Dapprich, S.; Millam, J. M.; Daniels, A. D.; Kudin, K. N.; Strain, M. C.; Farkas, O.; Tomasi, J.; Barone, V.; Cossi, M.; Cammi, R.; Mennucci, B.; Pomelli, C.; Adamo, C.; Clifford, S.; Ochterski, J.; Petersson, G. A.; Ayala, P. A.; Cui, Q.; Morokuma, K.; Salvador, P.; Dannenberg, J. J.; Malick, D. K.; Rabuck, A. D.; Raghavachari, K.; Foresman, J. B.; Cioslowski, J.; Ortiz, J. V.; Baboul, A. G.; Stefanov, B. B.; Liu, G.; Liashenko, A.; Piskorz, P.; Komaromi, I.; Gomperts, R.; Martin, R. L.; Fox, D. J.; Keith, T.; Al-Laham, M. A.; Peng, C. Y.; Nanayakkara, A.; Challacombe, M.; Gill, P. M. W.; Johnson, B. G.; Chen, W.; Wong, M. W.; Andres, J. L.; Gonzalez, C.; Head-Gordon, M.; Replogle, E. S.; Pople, J. A. GAUSSIAN03, Revision E.01, Gaussian, Inc., Wallingford CT, 2004.
16. MacDonald, D.; Herbert, K.; Zhang, X.; Polgruto, T.; Lu, P. *J. Mol. Biol.* **2001**, *306*, 1081.
17. Lewis, F. D.; Wu, T.; Zhang, Y.; Letsinger, R. L.; Greenfield, S. R.; Wasielewski, M. R. *Science* **1997**, *277*, 673.
18. Cardullo, R. A.; Agrawal, S.; Flores, C.; Zamecnik, P. C.; Wolf, D. E. *Proc. Natl. Acad. Sci. U.S.A.* **1988**, *85*, 8790.